Palladium-Catalyzed Annulation of Aryl-1,2-diols and Propargylic Carbonates. Theoretical Study of the Observed Regioselectivities

Jean-Robert Labrosse,[a] Paul Lhoste,[a] Françoise Delbecq,*[b,c] and Denis Sinou*[a]

Keywords: Annulation / Density functional calculations / Palladium / Regioselectivity

Methyl 1-methylprop-2-ynyl carbonate reacts with 3- and 4-substituted benzene-1,2-diols to give 2,3-dihydro-3-methyl-2-methylidene-1,4-benzodioxines, as a mixture of regioisomers in the case of methoxy-substituted diphenol, and a single regioisomer for the nitro- and the formyl-substituted diphenols. The oxyanion which attacks first corresponds to the less acidic hydroxy function, and the attack of the second oxyanion on the η^3-allylpalladium intermediate is directed toward the more substituted carbon atom. In order to explain the regioselectivity of the cyclization, a theoretical study based on density functional theory (DFT) has been performed. The first step implies an equilibrium between the two oxyanions. The regioselectivity of the second step is due to a subtle balance between the nature of the phosphane, the bulkiness, and the electronic properties of the substituents.

Introduction

Compounds containing the 1,4-benzodioxine and 1,4-benzodioxane structures exhibit interesting biological activities.[1−3] Various 2-substituted 1,4-benzodioxanes, for example, have shown properties as α- or β-blocking agents and have been used in antidepression or antihypertension therapy,[6−10] while others have exhibited antihyperglycemic properties[11] or acted as inhibitors of 5-lipoxygenase.[12] As a consequence, there has been increasing interest in their synthesis during the last years. Synthetic routes to 2-alkylidene-1,4-benzodioxanes are not straightforward and often need a tedious, multi-step sequence.[13−21] Our group has recently reported a very easy route to various 2-alkylidene-2,3-dihydro-1,4-benzodioxines through a palladium-catalyzed cyclization of propargylic carbonates with benzene-1,2-diols, even in an asymmetric fashion.[22−25] The mechanism proposed for this reaction was mainly based on studies published by different groups. In this paper we describe the extension of this methodology to substituted benzene-1,2-diols and a theoretical study to explain the different regio- and stereoselectivities observed in the cyclization producing 2-alkylidene-1,4-benzodioxine.

[a] Laboratoire de Synthèse Asymétrique, associé au CNRS, ESCPE Lyon, Université Claude Bernard Lyon 1,
43, boulevard du 11 novembre 1918, 69622 Villeurbanne Cedex, France
Fax: (internat.) +33(0)4-72448160
E-mail: sinou@univ-lyon1.fr
[b] Institut de Recherches sur la Catalyse,
2 avenue Einstein, 69626 Villeurbanne Cedex, France
Fax: (internat.) +33(0)4-72445399
E-mail: delbecq@catalyse.univ-lyon1.fr
[c] Laboratoire de Chimie Théorique et des Matériaux Hybrides, Ecole Normale Supérieure de Lyon,
46 allée d'Italie, 69364 Lyon Cédex 07, France
Fax: (internat.) +33(0)4 72445399
E-mail: delbecq@catalyse.univ-lyon1.fr

Results

In our previous papers concerning the palladium-catalyzed route to 2-alkylidene-1,4-benzodioxanes we only used benzene-1,2-diol (**1a**) as the diphenol (Scheme 1). We found that the cyclization process was often quite regio- and stereoselective, the major regioisomer being formed by intramolecular attack of the intermediate phenoxide ion on the more electrophilic terminus of the η^3-allylpalladium intermediate.[23] We also found that the stereochemistry of the double bond in the resulting heterocycle depended on the substitution pattern of the propargylic carbonate: primary and secondary carbonates afforded mainly the (*Z*) alkene, while tertiary carbonates gave predominantly the (*E*) isomer. We thought that it would be interesting to extend this methodology to substituted catechols, in order to obtain 2-alkylidene-2,3-dihydro-1,4-benzodioxines bearing various substituents on the phenyl ring. For this purpose, we choose methyl 1-methylprop-2-ynyl carbonate (**2**) as the propargylic carbonate, and catechols bearing electron-withdrawing or -donating groups at positions 3 or 4, namely 3-methoxybenzene-1,2-diol, 2,3-dihydroxybenzaldehyde, and 3-nitrobenzene-1,2-diol (**1b−d**), and 4-methoxybenzene-1,2-diol, 3,4-dihydroxybenzaldehyde, and 4-nitrobenzene-1,2-diol (**5a−c**) as the substituted diphenols. The condensation was performed as described previously,[23] in THF in the presence of the catalyst obtained by mixing $[Pd_2(dba)_3]$ and

dppb. The results of the cyclization are summarized in Table 1.

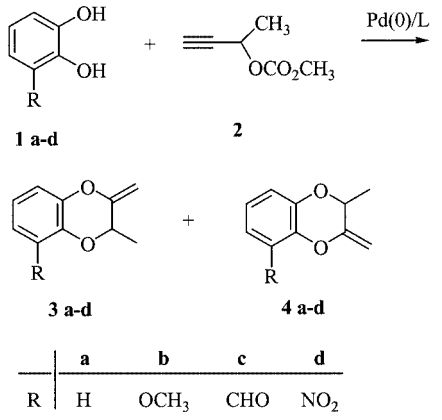

Scheme 1. Palladium(0)-catalyzed synthesis of compounds **3** and **4**

Table 1. Palladium(0)-catalyzed cyclization of carbonate **2** and diphenols **1** and **5**

Entry	Diphenol	Yield (%)	Regioisomers (%)
1	**1a**	99	–
2	**1b**	94	**3b** (50%) + **4b** (50%)
3	**1c**	96	**3c** (100%)
4	**1d**	85	**3d** (100%)
5	**5a**	92	**6a** (84%) + **7a** (16%)
6	**5b**	91	**7b** (100%)
7	**5c**	93	**7c** (100%)

Condensation of 3-methoxybenzene-1,2-diol (**1b**) with methyl 1-methylprop-2-ynylcarbonate (**2**) (Scheme 1) afforded a 50:50 mixture of the two regioisomers **3b** and **4b** in 94% yield (Table 1, Entry 2), while the condensations of 2,3-dihydroxybenzaldehyde (**1c**) or 3-nitrobenzene-1,2-diol (**1d**) each gave a unique regioisomer **3c** or **3d** in 96 and 85% yields, respectively (Table 1, Entries 3 and 4). While condensation of 4-methoxybenzene-1,2-diol (**5a**) (Scheme 2) gave a 84:16 mixture of the two regioisomers **6a** and **7a** in 92% yield (Table 1, Entry 5), 3,4-dihydroxybenzaldehyde (**5b**) and 4-nitrobenzene-1,2-diol (**5c**) again

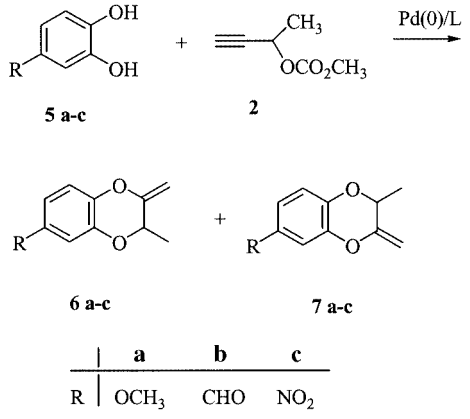

Scheme 2. Palladium(0)-catalyzed synthesis of compounds **6** and **7**

each gave a single regioisomer, namely **7b** and **7c**, in 91 and 93% yields, respectively (Table 1, Entries 6 and 7).

The structures of the regioisomers were determined by use of a HMBC sequence. For example, in the case of the compound arising from the condensation between 3-nitrobenzene-1,2-diol (**1d**) and methyl 1-methylprop-2-ynylcarbonate (**2**), the ^{13}C NMR shows four quaternary carbon atoms at δ = 138.8, 139.6, 144.1, and 152.7 ppm, corresponding to the carbon atoms of the aromatic ring near the oxygen and the nitro groups, the nitro group, the oxygen atom, and the carbon atom of the *exo*-double bond, respectively. We observed from the HMBC sequence that the signal of the carbon atom at δ = 138.8 ppm is coupled with the signal of the C-3 carbon atom at δ = 70.3 ppm, and that the signal of the carbon atom at δ = 144.1 ppm is also coupled with the $=CH_2$ signal at δ = 91.7 ppm; this is in agreement with structure **3d** for this compound.

According to Tsuji's work,[26] the reaction between propargylic carbonate **2** and palladium(0) generates the σ-allenylpalladium complex **A** and methanoate anion; attack of the monoanion of benzene-1,2-diol on the central sp carbon atom of this allenyl intermediate produces the palladium-carbene complexes **B** and **B′**, which are protonated by the secondary hydroxy function to give two η^1-allylpalladium intermediates in equilibrium with the two η^3-allylpalladium complexes **C** and **C′** (Scheme 3). Intramolecular nucleophilic attack on these η^3-allylpalladium complexes by the phenoxide gives the corresponding cyclized products. Another mechanism was proposed by Casey. Here, the σ−allenylpalladium complex **A** is in equilibrium with the σ-propargylpalladium intermediate **A′**.[27] Attack of the monoanion of benzene-1,2-diol at the central carbon atom of this propargylic ligand gives the metallacyclobutenes **D** and **D′**; further protonation of these metallacyclobutenes generates the η^3-allylpalladium complexes **C** and **C′**, giving rise to the cyclized compounds as previously shown. However, there is no clear evidence concerning either of these two mechanisms, and particularly on the nature of the complex obtained from the propargylic carbonate and the starting palladium(0) complex.

From a general mechanistic point of view, two steps in Scheme 3 give rise to questions. The first is the regioselectivity observed in the intramolecular nucleophilic attack by the phenoxide on the η^3-allylpalladium complex. In all cases, this attack occurred on the more substituted carbon atom or, better, on the more electrophilic atom of the η^3-allylcomplex, the attack on the less substituted carbon atom representing less than 5%. This means roughly 100% regioselectivity for the attack on the substituted carbon atom in the case of a methyl substituent, which is opposite to the usually reported regioselectivity,[28,29] but in agreement with the results of Larock et al. on similar systems.[30,31]

The second question is the regioselectivity of the attack of the catecholate anion on the σ-allenyl palladium complex in the case of substituted catechols. Which oxygen anion attacks first? The catecholate anion is formed by an acid-base reaction with the methanoate anion as shown in Scheme 4. The calculated pK_a values of the various cat-

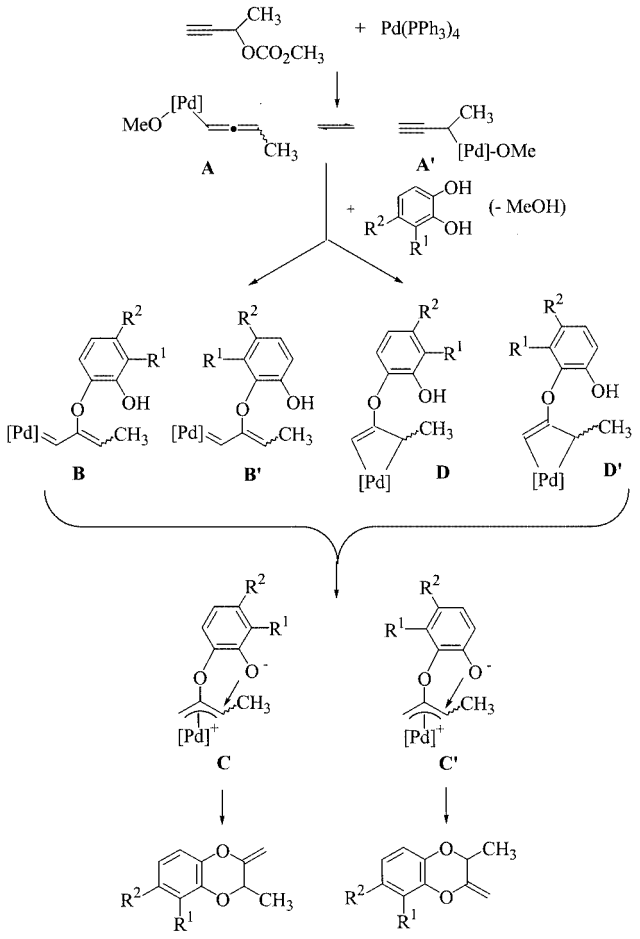

Scheme 3. Mechanism of formation of 2-alkylidene-2,3-dihydro-1,4-benzodioxines

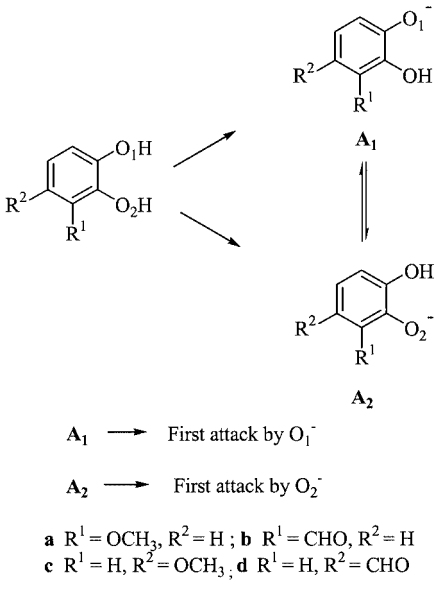

Scheme 4

echols in DMSO, obtained by use of the MOPAC program, are reported in Table 2. Table 2 also lists for each Entry the preferentially formed anion, following the pK_a order, and the anion attacking first according to the results contained in Table 1. It is to be noted that it is not the first formed anion that attacks first.

Table 2. pK_a values of substituted 1,2-benzenediols[a]

Entry	Diphenol	pK_a [a] O^1	O^2	Formed anion	Attacking anion (%)
2	**1b**	16	16	$\mathbf{A_1}/\mathbf{A_2}$	$\mathbf{A_1}/\mathbf{A_2}$ (50%/50%)
3	**1c**	14	12	$\mathbf{A_2}$	$\mathbf{A_1}$ (100%)
4	**1d**	12	8	$\mathbf{A_2}$	$\mathbf{A_1}$ (100%)
5	**5a**	17	16	$\mathbf{A_2}$	$\mathbf{A_1}/\mathbf{A_2}$ (84%/16%)
6	**5b**	13	14	$\mathbf{A_1}$	$\mathbf{A_2}$ (100%)
7	**5c**	9	12	$\mathbf{A_1}$	$\mathbf{A_2}$ (100%)

[a] Values were calculated by using the MOPAC program (DMSO as the solvent).

Theoretical Study

In order to provide a deeper insight into the reasons for the observed regioselectivity, we undertook a theoretical study on both the first attack and the second attack of the nucleophile. This study should also allow us better knowledge of the nature of the initial palladium complex.

Computational Methods

The calculations were based on the density functional theory (DFT) and performed with the aid of Gaussian 98.[32] The functional was B3LYP; two types of basis sets were used depending on the step studied. For the catecholate anions, we chose the base 6−31+G(d,p) (polarization functions on carbon, oxygen, hydrogen atoms, and diffuse functions, necessary for a good description of anions). On one example, for comparison, we also tested the Hartree−Fock method followed by a configuration interaction (HF + MP2). To study the reaction on the palladium complexes, the pseudo-potential of Hay and Wadt was used for palladium, with the double basis set of Dunning (LANL2DZ) augmented by polarization functions on carbon and oxygen atoms and one diffuse function on the anionic oxygen atoms.

All geometries were fully optimized, minima as well as maxima (transition states) on the potential energy curves. The natures of these extrema were verified by frequency calculations (0 or 1 imaginary frequency).

Solvent effects were introduced, since the reactions considered here are between charged species and are therefore sensitive to solvation, as we have already noticed previously.[29] The method used was Tomasi's Polarized Continuum Model (PCM).[33] The solvent considered was THF, as in the Exp. Sect. All the structures were reoptimized in the presence of solvent.

Study of the Catecholate Anions

We considered both the catecholate monoanion itself and catecholates substituted either with an electron-donating

group (OCH_3), or with an electron-withdrawing group (CHO), at two different positions (Scheme 4). To the best of our knowledge, some theoretical studies exist for the catechol[34] and the catecholate dianion,[35] but not for the monoanion. Various conformations for the hydroxy function were tested in the case of the catecholate anion without substituent ($R^1 = R^2 = H$). The conformation in which the hydrogen atom points towards O^- is the most stable, by 61 kJ·mol^{-1}, which reflects an important hydrogen bond. Hence, one can imagine that the catecholate anion could be a resonance form such as **8**, with the hydrogen atom at equal distances from the two oxygen atoms. In fact, such a structure is the transition state for the transfer of the hydrogen atom from one oxygen atom to the other; its geometry is given in Figure 1. The activation energy $\Delta E^{\#}$ is 20.3 kJ·mol^{-1} and the free activation energy $\Delta G^{\#}$ is 13.6 kJ·mol^{-1}. The barrier is small and so a rapid equilibrium exists between the two forms of the anion ($K_{eq} = 2.8 \times 10^{10}$ s^{-1}).

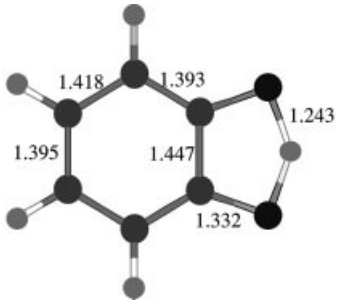

Figure 1. Geometry of the transition state connecting the two catecholate anions; bond lengths [A], oxygen atoms in dark gray, carbon atoms in medium gray, hydrogen atoms in light gray

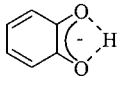

8

The four couples of catecholates **E**−**E′**, **F**−**F′**, **G**−**G′**, and **H**−**H′**, shown in Scheme 5, were then optimized. In each case, the best conformation of the substituent was searched for. The formyl group always remains in the molecular plane and adopts a conformation **E**−**E′** or **F**−**F′**, allowing a hydrogen bond. For the methoxy-substituted catechol, several conformations exist. The rotation around the C−O bond is almost free, with a barrier of 2.4 kJ·mol^{-1}. Nevertheless, the conformation **G′** or **H**−**H′**, in which the substituent OCH_3 is perpendicular to the molecular plane, is often the most stable. The energetic results are collected in Table 3. Firstly, the relative stability in each pair of anions is in agreement with the pK_a determination: the most stable anion corresponds to the deprotonation of the most acidic hydroxy function. The transition states allowing the transfer of the hydrogen atom from one oxygen atom to the other were searched for each catecholate, the activation free energy varying from 12 to 25 kJ·mol^{-1}. These small

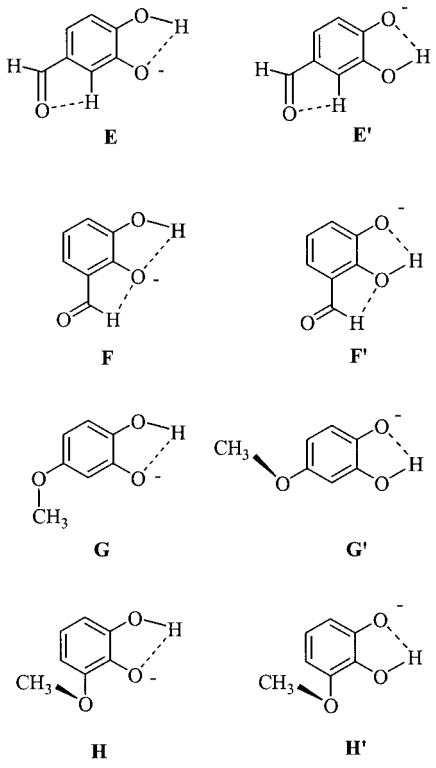

Scheme 5. Conformations of the catecholate anion

values allow us to assume that an easy equilibrium exists between each pair of anions at the reaction temperature.

Let us consider the charges on the anion. Both the Mulliken analysis and the natural population analysis have been used, and gave the same relative results. The major attack in each case corresponds to the anion bearing the greatest charge (Table 3). In the first case ($R^1 = OCH_3$ and $R^2 = H$), the charges are equivalent on $\mathbf{A_1}$ and $\mathbf{A_2}$, and a mixture of products is effectively observed. If the HOMOs (highest occupied molecular orbitals) are now considered, the major attack corresponds to that of the anion with the highest HOMO. Moreover, in this HOMO, the coefficient on the attacking oxygen atom is the largest one. The attack of the catecholate anion on the cationic palladium complex can be either charge-controlled or frontier orbital-controlled. In both cases, the anion which attacks first is the one bearing the greatest charge, the highest HOMO and the largest coefficient in the HOMO. However, whatever the substituent, this anion is the least stable. Therefore, in order to explain the experimentally obtained results, the reaction has to be assumed to be under kinetic control: the most stable anion, which is formed first, equilibrates to the second anion, which reacts more rapidly. We have seen just before that this equilibrium is easy.

The solvent effects were tested in the case of $R^1 = H$ and $R^2 = CHO$ with THF as the solvent. $\mathbf{A_1}$ remains more stable than $\mathbf{A_2}$ by $\Delta G = 18$ kJ·mol^{-1} and the $\Delta G^{\#}$ for the hydrogen transfer is 31 kJ·mol^{-1}. Both HOMOs are considerably stabilized, but remain in the same relative order. Moreover, the charges and the coefficients in the HOMO are not affected by the solvent. Hence the introduction of

Table 3. Relative electronic energies (E_{el}) and free energies at 298 K (G) of anions $\mathbf{A_1}$ and $\mathbf{A_2}$ and of the transition states between them, charge on the oxygen atoms (Q) by Mulliken analysis (Mul) or by Natural Bond Orbital Analysis (NBA), energy of the HOMO (E) and coefficients C on each oxygen atom in the HOMO, experimental majority attack, energies in kJ·mol^{-1}

Entry		Energy [kJ·mol^{-1}]				Q			HOMO		Attacking anion
		$\mathbf{A_1}$	**TS**	$\mathbf{A_2}$		$\mathbf{A_1}$	$\mathbf{A_2}$		$\mathbf{A_1}$	$\mathbf{A_2}$	(%)
2	E_{el}	0	20.2	0.2	Mul	−0.75	−0.74	E	−53	−50	$\mathbf{A_1}$/$\mathbf{A_2}$ (50%/50%)
	G	0	12.0	0.5	NBA	−0.82	−0.81	C	0.74	0.73	
3	E_{el}	18.5	29.4	0	Mul	−0.73	−0.69	E	−100	−118	$\mathbf{A_1}$ (100%)
	G	17.4	20.1	0	NBA	−0.77	−0.77	C	0.74	0.66	
5	E_{el}	5.1	21.8	0	Mul	−0.76	−0.74	E	−42	−51	$\mathbf{A_1}$/$\mathbf{A_2}$ (84%/16%)
	G	7.7	17.6	0	NBA	−0.83	−0.81	C	0.75	0.72	
6	E_{el}	0	34.5	23.8	Mul	−0.69	−0.73	E	−131	−108	$\mathbf{A_2}$ (100%)
	G	0	25.1	22.6	NBA	−0.76	−0.80	C	0.65	0.76	

the solvent effects decreases the reaction rate (HOMO more stable) but does not change the regioselectivity.

Study of the Palladium Complexes

The Allenyl/Propargyl Complex

As shown previously in Scheme 3, the palladium complex could be a σ-allenylcomplex **A** or a σ-propargylcomplex **A′** when the methoxy group is bound to the palladium atom. Decoordination of the methoxy group gives a cationic complex **I** (Scheme 6). When the geometry of this cationic complex **I** is optimized, it evolves spontaneously into an η^3-propargylic palladium complex with the triple bond coordinated to the metal. The structure is shown in Figure 2, and is a planar complex with a tetracoordinate palladium atom. The metal is bound to the terminal carbon atoms C^1 and C^3 with a longer bond for the substituted carbon atom (2.35 vs. 2.19 Å). The Pd−C^2 distance is short (2.19 Å), but there is no bond, since the overlap population is zero, in comparison with 0.17 and 0.14 between Pd and C^1 or C^3, respectively. Such a geometry for propargyl palladium complexes has been found experimentally and analyzed by X-ray spectroscopy.[36−38] Our optimized geometry is in good agreement with the experimentally ascertained ones. The same kind of structure has been obtained for propargyl/allenyl complexes of other metals such as Pt[36] and Re.[28] A molecular orbital description with Fenske−Hall and DFT calculations has been published in the case of the equivalent [(η^3-CH_2CCPh)Pt(PPh_3)$_2$].[39]

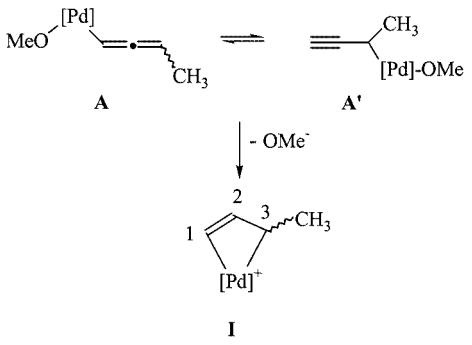

Scheme 6. Formation of the cationic complex **I**

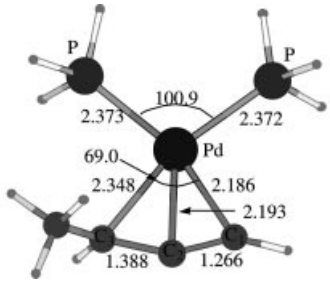

Figure 2. Geometry of the cationic allylic/propargylic complex **I**; bond lengths [Å], angles [°], carbon atoms in medium gray

Such allenyl/propargyl complexes are easily attacked by nucleophiles, including alcohols, amines, carbanions, etc. This attack always occurs at the central carbon atom,[39] as is also the case in this study. What are the reasons for this regioselectivity? Our DFT calculations, as well as the previous ones,[39] show that the central carbon atom C^2 is positively charged (+0.28), whereas the other carbon atoms are negatively charged (C^1: −0.42; C^3: −0.26). The LUMO of the complex is in the molecular plane, and has no contribution on the central carbon atom. Nevertheless, there is a higher vacant orbital with a large coefficient on the C^2 atom. Wojcicki et al.[40] concluded that the nucleophilic attack is charge-controlled. This conclusion is valid for charged nucleophiles such as carbanions, but could be questionable for neutral nucleophiles, or when the solvent is taken into account. For this reason we investigated this regioselectivity further. We used the semiempirical Hückel method (EHT) for studying the approach of two nucleophiles, NH_3 and OCH_3^-, towards **I** [(η^3-$CHCH_3CCH$)Pd(PH_3)$_2$]$^+$. This method gives the overlap populations between the carbon atoms of the complex and the attacking nucleophile, placed successively at the same distance from the three carbon atoms, and qualitatively indicates the preferred site of attack. Such a procedure has been successfully used in the past.[41,42] The results for the

attack of the nucleophile at a distance of 2.1 Å are given in Table 4. For both nucleophiles, the overlap population is positive and the largest on the central carbon atom, in agreement with an attack on this carbon atom. The overlap populations reflect the balance between attractive and repulsive interactions between orbitals. The regioselectivity can therefore also be explained by orbital interactions. We have constructed the interaction diagram for the attack of NH_3 on C^2 and on C^3 atoms, for which the overlap population is also positive. In the case of C^3 atom, we effectively observed the stabilizing interaction between the NH_3 lone pair and the LUMO, mostly located on this carbon atom. However this stabilization is counterbalanced by a destabilizing interaction with a complex occupied orbital also possessing a large coefficient on C^3 atom. There is no occupied orbital with a large coefficient on C^2 atom capable of acting with NH_3 in a destabilizing way and counterbalancing the weak interaction with the highest unoccupied orbital. Therefore, the nucleophilic attack on the central carbon C^2 atom of the allenyl/propargyl complex can also be viewed as orbital-controlled.

Table 4. Overlap populations between complex **I** and a nucleophile (NH_3, OMe^-) positioned at 2.1 Å from each carbon atom

C atom	NH_3	OMe^-
C^1	−0.06	−0.06
C^2	0.08	0.02
C^3	0.03	−0.02

The Palladacyclobutene

We next optimized the complex obtained by the attack of the nucleophile OH^- on the previous propargyl complex **I**, in order to model the attack of the catecholate anion to afford **D** or **D′** (Scheme 3). The geometry is shown in Figure 3. This is a planar palladacyclobutene: the C^1-C^2 bond length of 1.34 Å is consistent with a double bond. The OH bond is in the plane of the complex, which allows conjugation between the π system and the lone pair of the oxygen atom. Such metallacyclobutenes have been shown to be intermediates in the reactions between allenyl/propargyl complexes and nucleophiles such as NuH, giving allylic complexes.[43] X-ray structures have also been determined in the case of iridium[43] and platinum.[44] Our optimized values for the distances and the angles in the cycle are close to those obtained in the case of the platinum complex. The HOMO of the palladacyclobutene is the out-of-phase combination of π_{CC} and the oxygen p orbital with the largest coefficient on C^1 atom. With regard to the charges, C^2 atom is positively charged (+0.37), and C^1 and C^3 atoms are negatively charged (−0.48 and −0.29, respectively). The palladacyclobutene can therefore easily be attacked at C^1 atom by a proton to give an η^3-allylic palladium complex (Scheme 7), as observed experimentally.

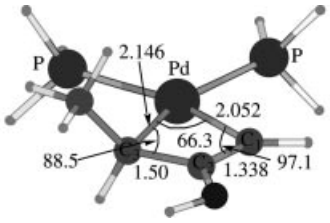

Figure 3. Geometry of the hydroxy-palladacyclobutene; bond lengths [Å], angles [°], carbon atoms in medium gray, oxygen atoms in dark gray

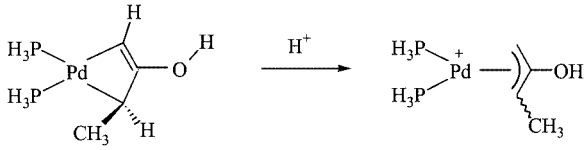

Scheme 7. Formation of the η^3-allylic palladium complex

In some cases, the transfer of the proton from the nucleophile NuH to the terminal carbon atom has been found to be stereospecific, the *syn* or *anti* conformation of the final η^3-allylic complex depending on the nature of the nucleophile (amine or alcohol).[36] Our case is different, since the proton adds to the nonsubstituted carbon atom C^1, whereas in the literature this carbon atom carries a substituent instead of a hydrogen atom. A question therefore arises: in which relative position, *cis* or *anti*, are the methyl group carried by C^3 and the catecholate part fixed on C^2? We will see further that this question is important for the determination of the stereoselectivity of the second step of the reaction, the attack of the second oxy anion on the η^3-allylic complex.

We therefore considered the true complex **9** obtained from the reaction between the catecholate anion and the allenyl/propargyl palladium complex. This corresponds to **D** and **D′** in Scheme 3 with $R^1 = R^2 = H$. The rotation around the C^2-O bond shows that the conformation in which C^2-O-C is in the plane of the complex is the most stable, as was the case with OH. The experimentalists believe that, at this stage of the reaction, there is no more base in the reaction medium and so the second hydroxy function of the catecholate is not ionized. The proton transfer is fairly concerted, as is assumed in the case of amines.[40] We therefore calculated the two structures **9a** and **9b** in which the hydrogen atom of the catecholate hydroxy approaches C^1 below and above the plane of the molecule (*trans* and *cis* relative to CH_3) (Figure 4). After optimization, we obtained two equivalent structures in which the C^1-H distance is 2.21 Å. A small positive overlap population exists between C^1 atom and the H atom (0.03) and the charges are −0.53 on C^1, +0.33 on the hydrogen and −0.41 on the oxygen atoms. These structures are therefore good precursors for the protonation of C^1 to afford an η^3-allylic palladium complex. The approach above C^1 atom forces C^2 atom to move below the plane of the complex, giving an η^3-allyl complex with the methyl and the catecholate *trans*

to each other (*anti* isomer). Contrarily, the approach below C^1 atom gives an η^3-allyl complex with the two substituents *cis* to each other (*syn* isomer). Since the two structures are energetically equivalent, the stereoselectivity cannot be determined in this way.

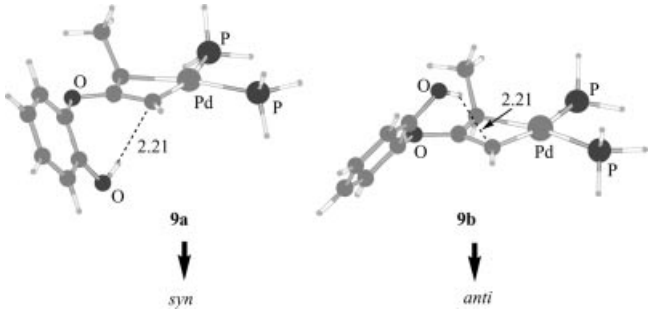

Figure 4. Optimized precursor complexes for the proton transfer to form the *syn* and the *anti* palladium allylic complexes

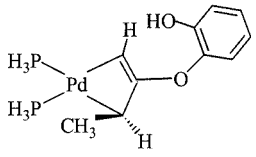

9

Let us now examine whether the stereoselectivity can be determined by thermodynamic arguments. For this purpose, we calculated the corresponding η^3-allylic complexes **10-*syn*** and **10-*anti***.

η^3-Allylpalladium Complexes

The geometries were first optimized by keeping the catecholate plane perpendicular to the allyl plane (Scheme 8).

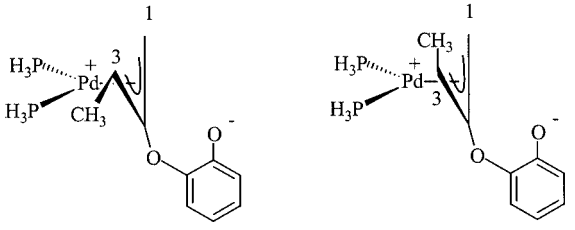

10-*syn*

10-*anti*

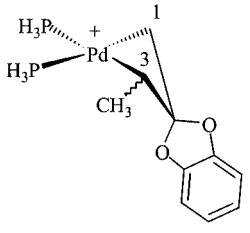

11

Scheme 8. Structures of the η^3-allylic palladium complexes

The **10-*syn*** complex is the more stable by 23 kJ·mol^{-1}, which is in favor of the formation of the *syn* complex. When the geometries are optimized without constraint, the oxygen atoms are bound to the central carbon C^2, giving a dioxygen cycle **11**, more stable than **10-*syn*** by 88 kJ·mol^{-1}. This is due to the fact that C^2 atom has a large positive charge and interacts easily with O^-through a purely electrostatic reaction.

We then optimized, without any constraints, the geometries obtained by rotation of the catecholate part in order to place O^- in proximity to C^1 or C^3 atoms, in the cases of *syn* and *anti* η^3-allyl palladium complexes **10**. We call these new complexes **10-*syn*-C^1**, **10-*syn*-C^3**, **10-*anti*-C^1**, and **10-*anti*-C^3**. Their relative energies are given in Table 5, together with their C−O distances. These complexes can be regarded as the precursor complexes for the reaction. Complex **10-*syn*-C^3** is difficult to optimize, due to its tendency to give the ring system **11** with two oxygen atoms through attack at C^2. If solvent effects are introduced (THF), this electrostatic interaction becomes weaker and the cyclic product with two oxygen atoms is not formed. We reoptimized the four precursor complexes taking the solvent effects into account; these results are also given in Table 5. Both in the presence and in the absence of THF, the best geometry is the *syn* one with the catecholate turned toward C^1 atom. The approach toward C^3 atom in the *syn* geometry is hindered by the methyl group. This is reflected by the larger C^3−O distance relative to C^1−O.

Table 5. Relative energies of the precursor complexes E, C−O distance *d* in these complexes, and activation energies relative to each precursor E$^{\#}$; first column: in vacuo, second column: with THF

Complex	*E* [kJ·mol^{-1}]		*d* C−O [Å]		$E^{\#}$ [kJ·mol^{-1}]	
	vacuum	THF	vacuum	THF	vacuum	THF
10-*syn*-C^1	0.0	0.0	2.57	2.84	3.4	26.5
10-*syn*-C^3	9.2	13.7	2.81	2.94	13.3	29.5
10-*anti*-C^1	14.9	12.3	2.59	2.83	3.5	26.7
10-*anti*-C^3	7.3	12.9	2.52	2.78	0.5	16.2

Nucleophilic Attack on the η^3-Allylpalladium Complex

We have calculated the four transition states (TSs) relating to the attack of the catecholate anion on C^1 and C^3 atoms for the *syn* and the *anti* isomers of the η^3-allyl palladium complexes. The results are given in Table 5. Firstly, one notices that the activation energies are very small in the absence of THF, which reflects the ease of the interaction between O^- and a cationic complex. The introduction of solvent effects in the calculation of the energy barriers is therefore necessary, although the method used is only qualitative. For the *syn* isomer, the smallest activation energy is found in the case of the attack on the less substituted carbon C^1. Conversely, for the *anti* isomer, the smallest activation energy is obtained in the case of the attack on the

more substituted carbon C^3. This is also by far the smallest of the four calculated values. However, we have seen that the most stable isomer is the *syn* one, so we must therefore implicate the less stable *anti* isomer in order to explain the regioselectivity toward C^3. The difference in the best activation energies between the *syn* and the *anti* isomers is large (10 kJ·mol^{-1}), and corresponds to a ratio of the kinetic constants of 1.3×10^4. Consequently, if an equilibrium exists between the *syn* and the *anti* isomers,[45−47] this equilibrium will be displaced toward the *anti* isomer by the far larger rate of its reaction.

In fact, experimentally, the regioselectivity also depends on the nature of the phosphane.[23] We therefore calculated the stabilities of the *syn* and the *anti* isomers of the η^3-methylallyl palladium complex **10** with PPh_3 and dppb [1,4-bis(diphenylphosphanyl)butane], respectively, as the ligand, instead of PH_3. For PPh_3, the *syn* isomer is more stable by 5 kJ·mol^{-1}, as in the case of PH_3. For dppb, in contrast, the *anti* isomer is the most stable by 9.6 kJ·mol^{-1}. Therefore, the relative stabilities of the *syn* and the *anti* isomers depend on the nature of the phosphane. This can be easily explained. In the *syn* isomer, the substituents on C^3 (methyl) and on C^2 (catecholate) atoms are in a *cis* position, so the relative stability comes from a balance between the steric hindrance between these two substituents in the *syn* isomer and the steric hindrance between the methyl and the phosphane ligands in the *anti* isomer. When the phosphorus atoms are linked by a carbon chain, the angle P−Pd−P decreases (106° for PH_3 and for PPh_3, 84° for dppb); so the phosphane moves away from CH_3 and releases the steric hindrance in the *anti* isomer. Experimentally, in the case of a methyl substituent on the η^3-allyl complex (case studied here), the phosphane used is dppb.[23] For this phosphane we have seen that the *anti* isomer is the most stable, and this is the reason why the reaction is so highly regioselective (more than 95% attach on C^3 atom).

It must be added that the regioselectivity of the nucleophilic attack on the η^3-allylpalladium complex also depends on the bulkiness of the substituents (steric effects) and on their electron-donor or -attractor character.[48] For example, when the methyl group is substituted by an ethyl, *tert*-butyl, or phenyl group, the attack on C^1 atom becomes more important.[23] In most cases, the product obtained has a (*Z*) stereochemistry on the double bond, which indicates that it is formed from the *syn* isomer. The regioselectivity of the reaction between catecholates and η^3-allylpalladium is therefore due to a balance of several factors: the relative stabilities of the *syn* and *anti* isomers of the complexes, the natures of the phosphanes, and the bulkiness and electronic character of the substituents of the η^3-allyl complex.

Conclusion

In this paper we have shown that methyl 1-methylprop-2-ynyl carbonate reacts with 3- and 4-substituted benzene-1,2-diols to give 2,3-dihydro-3-methyl-2-methylidene-1,4-benzodioxines, as a mixture of regioisomers in the case of methoxy-substituted diphenol, and as single regioisomers for the nitrodiphenols and the formyl-substituted diphenols.

A theoretical study has allowed us to obtain more insights into the mechanism of the palladium-catalyzed condensation of benzene-1,2-diols with propargyl carbonates. Two steps of the reaction were successively studied. With substituted catechols, the first question is the determination of the oxygen atom anion attacking the palladium complex. The calculations show that this anion corresponds to the less acidic hydroxy group and has the highest HOMO and the largest charge. A rapid equilibrium exists between the two possible anions.

The second step is the regioselective attack of the second oxygen atom anion on the η^3-allyl palladium complex. For this complex, the *syn* isomer is the most stable. However, it preferentially results in the attack on the less substituted carbon atom. In contrast, the *anti* isomer preferentially gives the attack on the most substituted carbon atom. Moreover, the relative stabilities of the *syn* and *anti* isomers depend on the natures of the phosphane ligands. With dppb [1,4-bis(diphenylphosphanyl)butane], the *anti* isomer is the most stable and this stability explains why the regioselectivity towards the attack on the substituted carbon atom is so high in the case of a methyl substituent. Finally, our calculations show that the direction of the reaction on the η^3-allyl palladium complex depends on several factors: the natures of the phosphanes, the bulkiness of the substituent on the allyl moiety, and its electronic character. The regioselectivity depends on the subtle balance between these factors and cannot be easily predicted.

Experimental Section

General Remarks: ^{1}H NMR (300 MHz) and ^{13}C NMR (50 MHz) spectra were obtained with a Bruker AM 300 spectrometer. Chemical shifts are reported as δ values with reference to $SiMe_4$ or $CDCl_3$ as an internal standard. The IR spectra were recorded with a Perkin−Elmer 681 instrument. All reactions were monitored by thin-layer chromatography carried out on 0.25 mm silica gel plates (60 F-254, Merck). Compounds were viewed under UV light (254 nm). Column chromatography was carried out on Merck silica gel 60 (40−63 μm). Reactions involving palladium complexes were carried out in a Schlenk tube under argon. Tetrahydrofuran was distilled from sodium−benzophenone and stored under argon. Compounds **1d**[49] and **5a**,[50] as well as methyl 1-methylprop-2-ynylcarbonate (**2**),[51] were prepared by literature procedures.

General Procedure for the Palladium-Catalyzed Annulation Reaction: A mixture of $[Pd_2(dba)_3]$ (20.8 mg, 2.2×10^{-2} mmol) and dppb (38.8 mg, 9.1×10^{-2} mmol) in THF (7 mL) was stirred under nitrogen at room temperature for 30 min. This catalyst solution was added to a mixture of aryl-1,2-diol (0.88 mmol) and methyl 1-methylprop-2-ynyl carbonate (128 mg, 1.0 mmol). The resulting solution was stirred at room temperature for 24 h. The solvent was evaporated and the residue was chromatographed over silica eluting with petroleum ether/ethyl acetate to afford the corresponding 2,3-dihydro-1,4-benzodioxine.

5-Methoxy-3-methyl-2-methylene-2,3-dihydro-1,4-benzodioxine (3b): 79 mg (in a 1:1 mixture of **3b** and **4b**), yield 47%. R_f = 0.22 (eluent: petroleum ether/ethyl acetate, 50:1). IR: $\tilde{\nu}$ = 3040, 980, 2930, 2820, 1650, 1590, 1485, 1460, 1250 cm^{-1}. ^{1}H NMR (300 MHz, $CDCl_3$): δ = 1.58 (d, J = 6.6 Hz, 3 H, CH_3), 3.85 (s, 3 H, OCH_3), 4.41 (d, J = 2.2 Hz, 1 H, $=CH_2$), 4.56 (q, J = 6.6 Hz, 1 H, 3-H), 4.72 (d,

J = 2.2 Hz, 1 H, =CH_2), 6.53 (dd, J = 8.1, 1.3 Hz, 1 H, $H_{arom.}$), 6.60 (dd, J = 8.1, 1.3 Hz, 1 H, $H_{arom.}$), 6.83 (t, J = 8.1 Hz, 1 H, $H_{arom.}$) ppm. ^{13}C NMR (50 MHz, $CDCl_3$): δ = 17.5 (CH_3), 56.2 (OCH_3), 69.4 (C-3), 89.9 (=CH_2), 105.4 ($C_{arom.}$), 109.3 ($C_{arom.}$), 121.4 ($C_{arom.}$), 132.9 ($C_{arom.}$), 143.4 ($C_{arom.}$), 149.4 ($C_{arom.}$), 154.2 (C-2) ppm.

5-Methoxy-2-methyl-3-methylene-2,3-dihydro-1,4-benzodioxine (4b): 79 mg (in a 1:1 mixture of **4b** and **3b**), yield 47%. R_f = 0.32 (eluent: petroleum ether/ethyl acetate, 50:1). IR: $\tilde{\nu}$ = 3040, 2980, 2930, 2820, 1650, 1585, 1460, 1250 cm^{-1}. ^{1}H NMR (300 MHz, $CDCl_3$): δ = 1.54 (d, J = 6.4 Hz, 3 H, CH_3), 3.88 (s, 3 H, OCH_3), 4.44 (d, J = 2.2 Hz, 1 H, =CH_2), 4.52 (q, J = 6.4 Hz, 1 H, H-2), 4.85 (d, J = 2.2 Hz, 1 H, =CH_2), 6.54 (d, J = 8.5 Hz, 2 H, $H_{arom.}$), 6.81 (t, J = 8.5 Hz, 1 H, $H_{arom.}$) ppm. ^{13}C NMR (50 MHz, $CDCl_3$): δ = 17.3 (CH_3), 56.2 (OCH_3), 69.1 (C-2), 90.3 (=CH_2), 105.0 ($C_{arom.}$), 110.0 ($C_{arom.}$), 121.1 ($C_{arom.}$), 132.2 ($C_{arom.}$), 143.9 ($C_{arom.}$), 148.0 ($C_{arom.}$), 153.8 (C-3) ppm. $C_{11}H_{12}O_3$ (192.22): calcd. C 68.72, H 6.30; found C 68.36, H 6.12.

3-Methyl-2-methylene-2,3-dihydro-1,4-benzodioxine-5-carbaldehyde (3c): 160 mg, yield 96%. R_f = 0.37 (eluent: petroleum ether/ethyl acetate, 10:1). M.p. 46−48 °C. IR: $\tilde{\nu}$ = 3050, 2980, 2920, 2850, 1670, 1660, 1580, 1470, 1270 cm^{-1}. ^{1}H NMR (300 MHz, $CDCl_3$): δ = 1.57 (d, J = 6.4 Hz, 3 H, CH_3), 4.47 (d, J = 2.0 Hz, 1 H, =CH_2), 4.62 (q, J = 6.4 Hz, 1 H, H-3), 4.77 (d, J = 2.0 Hz, 1 H, =CH_2), 6.93 (t, J = 7.9 Hz, 1 H, $H_{arom.}$), 7.13 (dd, J = 7.9, 1.5 Hz, 1 H, $H_{arom.}$), 7.40 (dd, J = 7.9, 1.5 Hz, 1 H, $H_{arom.}$), 10.38 (s, 1 H, CHO) ppm. ^{13}C NMR (50 MHz, $CDCl_3$): δ = 17.4 (CH_3), 69.8 (C-3), 91.1 (=CH_2), 121.0 ($C_{arom.}$), 121.6 ($C_{arom.}$), 121.8 ($C_{arom.}$), 125.5 ($C_{arom.}$), 143.2 ($C_{arom.}$), 146.2 ($C_{arom.}$), 153.3 (C-2), 188.9 (CHO) ppm. $C_{11}H_{10}O_3$ (190.20): calcd. C 69.45, H 5.30; found C 69.28, H 5.30.

3-Methyl-2-methylene-5-nitro-2,3-dihydro-1,4-benzodioxine (3d): 155 mg, yield 85%. R_f = 0.41 (eluent: petroleum ether/ethyl acetate, 10:1).). M.p. 65−68 °C. IR: $\tilde{\nu}$ = 3050, 2980, 2920, 1660, 1600, 1580, 1520, 1470, 1280 cm^{-1}. ^{1}H NMR (300 MHz, $CDCl_3$): δ = 1.61 (d, J = 6.4 Hz, 3 H, CH_3), 4.53 (d, J = 1.8 Hz, 1 H, =CH_2), 4.66 (q, J = 6.4 Hz, 1 H, H-3), 4.83 (d, J = 1.8 Hz, 1 H, =CH_2), 6.96 (t, J = 8.1 Hz, 1 H, $H_{arom.}$), 7.18 (dd, J = 8.1, 1.3 Hz, 1 H, $H_{arom.}$), 7.54 (dd, J = 8.1, 1.3 Hz, 1 H, $H_{arom.}$) ppm. ^{13}C NMR (50 MHz, $CDCl_3$): δ = 17.3 (CH_3), 70.3 (C-3), 91.7 (=CH_2), 118.7 ($C_{arom.}$), 121.1 ($C_{arom.}$), 121.3 ($C_{arom.}$), 138.8 ($C_{arom.}$), 139.6 ($C_{arom.}$), 144.1 ($C_{arom.}$), 152.7 (C-2) ppm. $C_{10}H_9NO_3$ (207.19): calcd. C 57.96, H 4.38; found C 57.76, H 4.45.

6-Methoxy-3-methyl-2-methylene-2,3-dihydro-1,4-benzodioxine (6a): 130 mg (in a 84:16 mixture of **6a** and **7a**), yield 77%. R_f = 0.15 (eluent: petroleum ether/ethyl acetate, 50:1). IR: $\tilde{\nu}$ = 3030, 2980, 2920, 2820, 1660, 1610, 1590, 1500, 1440, 1250 cm^{-1}. ^{1}H NMR (300 MHz, $CDCl_3$): δ = 1.50 (d, J = 6.5 Hz, 3 H, CH_3), 3.70 (s, 3 H, OCH_3), 4.37 (d, J = 1.8 Hz, 1 H, =CH_2), 4.52 (q, J = 6.5 Hz, 1 H, H-3), 4.68 (d, J = 1.8 Hz, 1 H, =CH_2), 6.43−6.88 (m, 3 H, $H_{arom.}$) ppm. ^{13}C NMR (50 MHz, $CDCl_3$): δ = 17.4 (CH_3), 55.7 (OCH_3), 69.4 (C-3), 89.3 (=CH_2), 102.8 ($C_{arom.}$), 107.7 ($C_{arom.}$), 116.2 ($C_{arom.}$), 137.0 ($C_{arom.}$), 143.7 ($C_{arom.}$), 154.6 ($C_{arom.}$), 154.8 (C-2) ppm. $C_{11}H_{12}O_3$ (192.22): calcd. C 68.72, H 6.30; found C 68.75, H 6.28.

6-Methoxy-2-methyl-3-methylene-2,3-dihydro-1,4-benzodioxine (7a): 26 mg (in a 16:84 mixture of **6a** and **7a**), yield 15%). R_f = 0.15 (eluent: petroleum ether/ethyl acetate, 50:1). IR: $\tilde{\nu}$ = 3040, 2980, 2930, 2820, 1650, 1585, 1460, 1250 cm^{-1}. ^{1}H NMR (300 MHz, $CDCl_3$): δ = 1.48 (d, J = 6.5 Hz, 3 H, CH_3), 3.72 (s, 3 H, OCH_3), 4.40 (d, J = 1.8 Hz, 1 H, =CH_2), 4.47 (q, J = 6.5 Hz, 1 H, H-2), 4.72 (d, J = 1.8 Hz, 1 H, =CH_2), 6.43−6.88 (m, 3 H, $H_{arom.}$) ppm. ^{13}C NMR (50 MHz, $CDCl_3$): δ = 17.3 (CH_3), 55.8 (OCH_3), 69.1 (C-2), 89.7 (=CH_2), 101.8 ($C_{arom.}$), 107.8 ($C_{arom.}$), 117.3 ($C_{arom.}$), 137.5 ($C_{arom.}$), 143.1 ($C_{arom.}$), 155.2 ($C_{arom.}$), 155.4 (C-3) ppm.

2,3-Dihydro-2-methyl-3-methylene-2,3-dihydro-1,4-benzodioxine-6-carbaldehyde (7b): 152 mg, yield 91%. R_f = 0.28 (eluent: petroleum ether/ethyl acetate, 10:1). M.p. 46−48 °C. IR: $\tilde{\nu}$ = 3050, 2980, 2930, 2820, 1675, 1650, 1575, 1490, 1430, 1260 cm^{-1}. ^{1}H NMR (300 MHz, $CDCl_3$): δ = 1.57 (d, J = 6.4 Hz, 3 H, CH_3), 4.47 (br. s, 1 H, =CH_2), 4.62 (q, J = 6.4 Hz, 1 H, H-2), 4.76 (br. s, 1 H, =CH_2), 6.95 (t, J = 8.1 Hz, 1 H, $H_{arom.}$), 7.40 (dd, J = 8.1, 1.5 Hz, 1 H, $H_{arom.}$), 7.41 (s, 1 H, $H_{arom.}$), 9.80 (s, 1 H, CHO) ppm. ^{13}C NMR (50 MHz, $CDCl_3$): δ = 17.4 (CH_3), 69.7 (C-2), 91.4 (=CH_2), 117.0 ($C_{arom.}$), 117.8 ($C_{arom.}$), 125.0 ($C_{arom.}$), 131.2 ($C_{arom.}$), 142.7 ($C_{arom.}$), 148.5 ($C_{arom.}$), 152.9 (C-3), 190.5 (CHO) ppm. $C_{11}H_{10}O_3$ (190.20): calcd. C 69.45, H 5.30; found C 69.42, H 5.25.

2-Methyl-3-methylene-6-nitro-2,3-dihydro-1,4-benzodioxine (7c): 169 mg, yield 93%. R_f = 0.35 (eluent: petroleum ether/ethyl acetate, 10:1). M.p. 53−55 °C. IR: $\tilde{\nu}$ = 3080, 3050, 2980, 2910, 2840, 1655, 1585, 1515, 1485, 1425, 1340, 1270 cm^{-1}. ^{1}H NMR (300 MHz, $CDCl_3$): δ = 1.52 (d, J = 6.4 Hz, 3 H, CH_3), 4.53 (d, J = 2.0 Hz, 1 H, =CH_2), 4.60 (q, J = 6.4 Hz, 1 H, H-2), 4.83 (d, J = 2.0 Hz, 1 H, =CH_2), 6.93 (t, J = 8.4 Hz, 1 H, $H_{arom.}$), 7.77 (s, 1 H, $H_{arom.}$), 7.78 (d, J = 8.4 Hz, 1 H, $H_{arom.}$). ^{13}C NMR (50 MHz, $CDCl_3$): δ = 17.3 (CH_3), 69.9 (C-2), 92.2 (=CH_2), 112.3 ($C_{arom.}$), 117.3 ($C_{arom.}$), 118.2 ($C_{arom.}$), 141.9 ($C_{arom.}$), 142.8 ($C_{arom.}$), 148.7 ($C_{arom.}$), 152.3 (C-3) ppm. $C_{10}H_9NO_3$ (207.19): calcd. C 57.96, H 4.38; found C 57.70, H 4.27.

Acknowledgments

One of us (J. R. L.) thanks the French Ministry of Education for a fellowship. F. D. thanks the Centre Informatique National de l'Enseignement Supérieur (CINES) at Montpellier for CPU time.

[1] L. Merlini, A. Zanarotti, A. Pelter, M. P. Rochefort, R. Haensel, *J. Chem. Soc., Chem. Commun.* **1979**, 695.
[2] A. Arnone, L. Merlini, A. Zanarotti, *J. Chem. Soc., Chem. Comun.* **1979**, 696−697.
[3] P. Bosseray, G. Guillaumet, G. Coudert, H. Wasserman, *Tetrahedron Lett.* **1989**, *30*, 1387−1390.
[4] S. L. Debenedetti, E. L. Nadinic, J. D. Coussio, N. de Kimpe, J. F. Dupont, J. P. Declercq, *Phytochemistry* **1991**, *30*, 2757−2758.
[5] S. Tsukamoto, H. Kato, H. Hirota, N. Fusetani, *Tetrahedron* **1994**, *50*, 13583−13592.
[6] W. L. Nelson, J. E. Wennerstrom, D. C. Dyer, J. E. Engel, *J. Med. Chem.* **1977**, *20*, 880−885.
[7] G. Marciniak, A. Delgado, G. Leclerc, J. Velly, N. Decker, J. Schwartz, *J. Med. Chem.* **1989**, *32*, 1402−1407.
[8] R. R. Ruffolo, Jr., W. Bondinell, J. P. Hieble, *J. Med. Chem.* **1995**, *38*, 3681−3716.
[9] D. Giardina, R. Bertini, E. Brancia, L. Brasili, C. Melchiorre, *J. Med. Chem.* **1985**, *28*, 1354−1357.
[10] W. Quaglia, M. Pigini, S. K. Tayebati, A. Piergentili, M. Gianella, A. Leornadi, C. Taddei, C. Melchiorre, *J. Med. Chem.* **1996**, *39*, 2253−2258.
[11] G. P. Fagan, C. P. Chapleo, A. C. Lane, M. Myers, C. F. C. Roach, M. R. Stillings, A. P. Welbourn, *J. Med. Chem.* **1988**, *31*, 944−948.
[12] Y. Satoh, C. Powers, L. M. Toledo, T. J. Kowalski, P. A. Peters, E. F. Kimble, *J. Med. Chem.* **1995**, *38*, 68−75.
[13] M. Yamamoto, *J. Chem. Soc., Perkin Trans. 1* **1979**, 3161−3165.

[14] S. Cabiddu, C. Floris, S. Melis, F. Sotgiu, G. Cerioni, *J. Heterocycl. Chem.* **1986**, *23*, 1815−1820.
[15] V. Rosnati, A. Salimbeni, *Tetrahedron* **1986**, *42*, 4541−4548.
[16] N. Ruiz, P. Rollin, *Tetrahedron Lett.* **1989**, *30*, 1637−1640.
[17] P. Moreau, M. Al Neirabeyeh, G. Guillaumet, G. Coudert, *Tetrahedron Lett.* **1991**, *32*, 5525−5528.
[18] A. Basak, G. Bhattacharya, U. K. Mallik, U. K. Khamrai, *Synthetic Commun.* **1997**, *27*, 367−373.
[19] C. Chowdhury, N. G. Kundu, *Chem. Commun.* **1996**, 1067−1068.
[20] M. G. Organ, M. Miller, Z. Konstantinou, *J. Am. Chem. Soc.* 1998, *120*, 9283−9290.
[21] C. Chowdhury, G. Chaudhuri, S. Guha, A. K. Mukherjee, N. G. Kundu, *J. Org. Chem.* **1998**, *63*, 1863−1871.
[22] J. R. Labrosse, P. Lhoste, D. Sinou, *Tetrahedron Lett.* **1999**, *40*, 9025−9028.
[23] J. R. Labrosse, P. Lhoste, D. Sinou, *J. Org. Chem.* **2001**, *66*, 6634−6642.
[24] J. R. Labrosse, P. Lhoste, D. Sinou, *Eur. J. Org. Chem.* **2002**, 1966−1971.
[25] J. R. Labrosse, P. Lhoste, D. Sinou, *Organic Lett.* **2000**, *2*, 527−529.
[26] T. Mandai, J. Tsuji, *Angew. Chem.* **1995**, *107*, 2830−2854; *Angew. Chem. Int. Ed. Engl.* **1995**, *34*, 2589−2612.
[27] C. P. Casey, J. R. Nash, C. S. Yi, A. D. Selmeczy, S. Chung, D. R. Powell, R. K. Hayashi, *J. Am. Chem. Soc.* **1998**, *120*, 722−733.
[28] [28a] B. M. Trost, D. L. Van Vranken, *Chem. Rev.* **1996**, *96*, 395−422. [28b] B. M. Trost, R. C. Bunt, *J. Am. Chem. Soc.* **1998**, *120*, 70−79.
[29] F. Delbecq, C. Lapouge, *Organometallics* **2000**, *19*, 2716−2723.
[30] R. C. Larock, Y. He, W. W. Leong, X. Han, M. D. Refvik, J. M. Zenner, *J. Org. Chem.* **1998**, *63*, 2154−2160.
[31] R. C. Larock, C. Tu, P. Pace, *J. Org. Chem.* **1998**, *63*, 6859−6866.
[32] Gaussian 98 (Revision A.7), M. J. Frisch, G. W. Trucks, H. B. Schlegel, G. E. Scuseria, M. A. Robb, J. R. Cheeseman, V. G. Zakrzewski, J. A. Montgomery, R. E. Stratmann, J. C. Burant, S. Dapprich, J. M. Millam, A. D. Daniels, K. N. Kudin, M. C. Strain, O. Farkas, J. Tomasi, V. Barone, M. Cossi, R. Cammi, B. Mennucci, C. Pomelli, C. Adamo, S. Clifford, J. Ochterski, G. A. Petersson, P. Y. Ayala, Q. Cui, K. Morokuma, D. Malick, A. D. Rabuck, K. Raghavachari, J. B. Foresman, J. Cioslowski, J. V. Ortiz, B. B. Stefanov, G. Liu, A. Liashenko, P. Piskorz, I. Komaromi, R. Gomperts, R. L. Martin, D. J. Fox, T. Keith, M. A. Al-Laham, C. Y. Peng, A. Nanayakkara, C. Gonzalez, M. Challlacombe, P. M. W. Gill, B. G. Johnson, W. Chen, M. W. Wong, J. L. Andres, M. Head-Gordon, E. S. Replogle, J. A. Pople, Gaussian, Inc., Pittsburgh PA, 1998.
[33] J. Tomasi, M. Persico, *Chem. Rev.* **1994**, *94*, 2027−2094.
[34] M. Gerhards, S. Schumm, C. Unterberg, K. Kleinermanns, *Chem. Phys. Lett.* **1998**, *294*, 65−70.
[35] D. E. Wheeler, J. H. Rodriguez, J. K. Mc Cusker, *J. Phys. Chem.* **1999**, *103*, 4101−4112.
[36] M. W. Baize, P. W. Blosser, V. Plantevin, D. G. Schimpff, J. C. Gallucci, A. Wojcicki, *Organometallics* **1996**, *15*, 164−173.
[37] S. Ogoshi, K. Tsutsumi, H. Kurosawa, *J. Organomet. Chem.* **1995**, *493*, C15−C21.
[38] K. Tsutsumi, S. Ogoshi, S. Nishiguchi, H. Kurosawa, *J. Am. Chem. Soc.* **1998**, *120*, 1938−1939.
[39] J. P. Graham, A. Wojcicki, B. E. Bursten, *Organometallics* **1999**, *18*, 837−842.
[40] A. Wojcicki, *Inorg. Chem. Commun.* **2002**, 5, 82−97.
[41] B. E. R. Shilling, R. Hoffmann, J. W. Faller, *J. Am. Chem. Soc.* **1979**, *101*, 592−598.
[42] F. Delbecq, B. Bigot, *New. J. Chem.* **1990**, *14*, 659−669.
[43] Y.-C. Cheng, Y.-K. Cheng, T.-M. Huang, C.-I. Yu, G.-H. Lee, Y. Wang, C.-T. Chen, *Organometallics* **1998**, *17*, 2953−2957.
[44] R. C. Hemond, R. P. Hughes, D. J. Robinson, A. L. Rheingold, *Organometallics* **1988**, *7*, 2239−2241.
[45] B. Akermark, S. Hansson, A. Vitagliano, *J. Am. Chem. Soc.* **1990**, *112*, 4587−4588.
[46] M. Sjögren, S. Hansson, P.-O. Norrby, B. Akermark, M. E. Cucciolito, A. Vitagliano, *Organometallics* **1991**, *11*, 3954−3964.
[47] A. Togni, U. Burkhardt, V. Gramlich, P. Pregosin, R. Salzmann, *J. Am. Chem. Soc.* **1996**, *118*, 1031−1037.
[48] V. Branchadell, M. Moreno-Mañas, F. Pajuelo, R. Pleixats, *Organometallics* **1999**, *18*, 4934−4941.
[49] R. C. Cambie, G. R. Clark, S. L. Coombe, S. A. Coulson, P. S. Rutledge, P. D. Woodgate, *J. Organomet. Chem.* **1996**, 507, 1−21.
[50] K. Aihara, Y. Urano, T. Higuchi, M. Hirobe, *J. Chem. Soc., Perkin Trans. 2* **1993**, 2165−2170.
[51] G. W. Gribble, H. H. Joyner, F. L. Switzer, *Synth. Commun.* **1992**, *22*, 2997−3002.

Received February 6, 2003

